C. R. Mecanique 340 (2012) 485–492

Contents lists available at SciVerse ScienceDirect

Comptes Rendus Mecanique

www.sciencedirect.com

Analytical and innovative solutions for heat transfer problems involving phase change and interfaces

The heat-balance integral: 1. How to calibrate the parabolic profile?

Jordan Hristov

Department of Chemical Engineering, University of Chemical Technology and Metallurgy, 1756 Sofia, 8 Kl. Ohridsky Blvd., Bulgaria

ARTICLE INFO

Article history:
Available online 3 May 2012

Keywords:
Heat-balance integral method
Entropy generation minimization
Myers approach
Half-time fractional derivative

ABSTRACT

The Heat-Balance Integral Method (HBIM) of Goodman under classic prescribed temperature boundary conditions has been studied towards it optimization. Because the parabolic profile satisfies both the boundary conditions and the heat-balance integral at any value of the exponent the calibration is of a primary importance in generation of the approximate solution. The simple 1-D heat conduction problem, enabling one to demonstrate the HBIM performance with the entropy generation minimization (EGM) concept in calibration of a parabolic temperature profile with unspecified exponents, has been developed. The EGM concept provides constraints that impose addition boundary conditions at the approximate parabolic profile. Additionally, entire domain optimizations based on the mean-squared error concept has been performed in two versions – the method Myers and through a similarity transformed diffusion equation.

1. Introduction

The heat balance integral method of Goodman [1] is an effective method for solving heat diffusion problems with strong non-linearity either in the energy equation or at the boundaries. Analytical solutions are, however, quite cumbersome and there cases where approximate simple analytical solutions are need. The Goodman method is one of the leading approaches among the approximate methods in solving 1-D transient diffusion problem over 50 years and it is still being under development [2–9]. The basic idea of the Heat-Balance Integral Method (HBIM) employs a physically-based formulation of a thermal layer (this avoids the physical inadequacy of the Fourier equation) and a prescribed temperature profile. These essential ideas allow transformation of strong non-linear 1-D heat conduction problems into ordinary differential equation with respect to the thermal layer temperature evolution [1,10]. The common approach is to use polynomial temperature approximations with respect to the space co-ordinate with up to 4 boundary conditions allowing defining the profile coefficients as functions of the thermal layer depth $\delta(t)$ (see Eqs. (3), too), namely:

$$T(0,t) = T_s \quad \text{or} \quad -\lambda\frac{\partial T}{\partial x} = \dot{q}_s \tag{1a}$$

$$T(\delta,t) = T_\infty \tag{1b}$$

$$\lambda\frac{\partial T}{\partial x}\bigg|_{x=\delta} = 0 \tag{1c}$$

$$\frac{\partial^2 T}{\partial x^2}\bigg|_{x=\delta} = 0 \tag{1d}$$

E-mail address: jordan.hristov@mail.bg.

1631-0721/$ – see front matter
doi:10.1016/j.crme.2012.03.001

Nomenclature

a	Term in the generalized parabolic profile (Eq. (4))
b	coefficient in the generalized parabolic profile (Eq. (4))
c	coefficient in the generalized parabolic profile (Eq. (4))
$E_n(n,t)$	mean-squared error of approximation defined by Eq. (19a)
$e_n(n,t)$	mean-squared error of approximation defined by Eq. (19b)
n	exponent of the parabolic profile
n_M^T	exponent defined by the Myers' method
q	heat flux density, W/m^2
q_s''	surface heat flux ($x=0$), W/m^2
S	entropy generation rate, W/K
T	temperature, K
T_a	approximate profile
T_∞	temperature of the undisturbed medium, K
t	time, s
x	space co-ordinate, m

Greek letters

α	thermal diffusivity, m^2/s
δ	thermal penetration depth, m
$\eta = x/\sqrt{\alpha t}$	similarity variable
λ	thermal conductivity, W/m K
Θ	dimensionless temperature

Subscripts

0	defined at the surface ($x=0$)
a	approximate
e	exact
M	Myers' method
s	surface (at $x=0$)
η	similarity method

Superscripts

T	prescribed temperature problem
q	prescribed flux problem

$$\delta(t=0)=0 \tag{2}$$

where $\delta(t)$ is the depth of the thermal penetration layer; the crux of the Goodman's method [1,2].

The conditions (1a) and (1b) are classical for the prescribed temperature and prescribed flux problems, respectively. The fourth condition (1d) is known as "smoothing condition" and works well when a polynomial approximation of 4th order is used. Generally, the accuracy of the HBIM depends on the adequate choice of the approximating functions and the literature provides many examples of successful solutions [11–15]. The present work addresses HBIM solution of heat–conduction problems in a semi-infinite solid under various prescribed conditions at the boundary $x=0$

$$\frac{\partial T(x,t)}{\partial t} = \alpha \frac{\partial^2 T(x,t)}{\partial x^2} \tag{3a}$$

$$0 \leqslant x \leqslant \delta(t) \tag{3b}$$

by a preliminarily defined parabolic profile $T_a(x,t)$ with unspecified exponent, namely

$$T_a(x,t) = a + b(1+cx)^n \tag{4}$$

The profile (3b) is very often used in the form (with $T_a(0,t)=T_s$)

$$\Theta = \frac{T(x,t)-T_\infty}{T_s-T_\infty} = \left(1-\frac{x}{\delta}\right)^n \tag{5}$$

Recently examples and analyses were provided by [13] where a clear algorithm defining the exponent n through additional constraints based on existing exact solutions was developed. This algorithm [13] allowed results developed by other methods [14] for solving (3a), (3b)–(5) to be obtained easily. Recently Myers [15] has suggested an improving mechanism of HBIM with the profile (3c) through mean-squared error minimization developing the Langford criterion [16].

(1) Regarding the profile (4), it was established [13], that if an additional boundary condition could be provided at $x=0$, then the exponent n can be directly defined. This implies, for instance, that in the case of prescribed temperature at $x=0$ (isothermal condition) the second condition needed is the flux, i.e. the derivative $(\partial T/\partial x)$ has to be known and whilst with a prescribed flux $q''(x=0) = -\lambda(\partial T/\partial x)_{x=0}$ the missing condition is the surface temperature $T_s(x=0)$. It was demonstrated by Hristov [13] that when either T_s or $q''(x=0)$ are *time-independent* a possible step to find the missing boundary condition is to use the exact solutions [17] at $x=0$. To avoid this problem, in the context of calibrating the profile (4), a general approach defining the missing boundary condition was conceived [18] through the *Entropy Generation Minimization* (EGM) constraint. The method was simply tested with problems having exact solutions [18]. The present work addresses the EGM method through definition of the missing boundary condition and providing it through fractional half-time derivative (integral) at $x=0$ of the prescribed temperature (flux) in the Riemann–Liouville sense.

2. Calibration of the profile at $x = 0$

2.1. EGM constraint and the fractional half-time derivative approach

If the temperature profile $T(x)$ is known then the local thermal entropy generation (TEG) rate $\dot{S}$, in absence of volumetric heat generation [19] is

$$\dot{S} = \frac{\lambda}{T^2}(\operatorname{grad} T)^2, \qquad T_x = \frac{\partial T}{\partial x} \tag{6}$$

The new thermodynamic constraint conceived [18] is that TEG calculated either by the exact or the approximate solution should be equal, that requires $\Delta\dot{S} = [\dot{S}(T, T_x)_a - \dot{S}(T, T_x)_e] \to \min$. The local approach at $x = 0$ with the strong condition $\Delta\dot{S} = 0$ defines $(\partial T/\partial x)_{a(x=0)}/T^2_{a(x=0)} = (\partial T/\partial x)_{e(x=0)}/T^2_{e(x=0)}$.

Then, if the heat flux $q''_s(x = 0) = -\lambda(\partial T/\partial x)$ is prescribed at $x = 0$, then we need $T_{a(x=0)} = T_{e(x=0)}$.

Otherwise, with isothermal surface condition $T_{a(x=0)} = T_{e(x=0)}$, the condition $\Delta\dot{S} = 0$ provides $(\partial T/\partial x)_{a(x=0)} = (\partial T/\partial x)_{e(x=0)}$. These conditions are general and valid for either independent or time-dependent boundary conditions.

Answering the principle question" *How to define an almost exact solution providing the missing boundary condition?*" we refer to fractional solutions of the heat equation (3) (see [20]). More precisely we are interested in the derivation of the flux at the boundary with prescribed temperature and *vice versa* by a Half-time Derivative Approach (HTA) if the local condition has to be satisfied. The benchmark solutions developed next briefly exemplify the method. Following the results of Kulish and Lage [21] we have the following solutions of the 1-D heat-conduction equation in a semi-infinite domain expressed through half-time fractional derivatives

$$q''_s(0, t) = \frac{\lambda}{\sqrt{\alpha}}\left[\frac{\partial^{1/2}T(0, t)}{\partial t^{1/2}} - \frac{T_\infty}{\sqrt{\pi t}}\right], \quad \text{with } T_{(x=0)} = T_s \tag{7}$$

$$T(0, t) = \frac{\sqrt{\alpha}}{\lambda}\frac{\partial^{-1/2}[q''_s(0, t)]}{\partial t^{-1/2}} + T_\infty, \quad \text{with } -\lambda\frac{\partial T}{\partial x}\bigg|_{x=0} = q''_s(t) \tag{8}$$

The relationships (7) and (8) are global and valid over the entire semi-infinite domain. Hence, the boundary values at $x = 0$, following from (8) provides local relationships namely [22]:

$$q''_s(t) = q''_s(0, t) = \frac{\lambda}{\sqrt{\alpha t}}\frac{1}{\sqrt{\pi}}(T_s - T_\infty) \tag{9a}$$

$$T_s = T(0, t) = 2q''_s(0, t)\frac{\sqrt{\alpha t}}{\lambda\sqrt{\pi}} + T_\infty \tag{9b}$$

These results are exactly the same as those obtained by exact solutions [17] (see comments in [18], too). Hence, with (9a) or (9b) the additional boundary condition needed to calibrate the approximate profile (at $x = 0$) is provided. The operators $\partial^{1/2}/t^{1/2}$ and $\partial^{-1/2}/t^{-1/2}$are half-time fractional derivative and integral in the Riemann–Liouville sense [20,22], namely

$$D_t^{1/2} = \frac{\partial^{1/2}T(x, t)}{\partial_+ t^{1/2}} = \frac{1}{\Gamma(1/2)}\frac{\mathrm{d}}{\mathrm{d}t}\int_0^t \frac{T(x, u)}{\sqrt{t - u}}\,\mathrm{d}u \tag{10}$$

were u is a dummy variable.

2.2. Benchmark solutions

2.3. Example 1. Prescribed temperature problem (PT) at $x = 0$, $T_s(0, t)) = const$

The HBIM solution of (3a) with $T = T_s$ at $x = 0$ and $T(x, 0) = T_\infty$, is [13]

$$T_a(x, t) = T_\infty + (T_s - T_\infty)\left(1 - \frac{x}{\sqrt{at}\sqrt{2n(n + 1)}}\right)^n \tag{11a}$$

$$\delta = \sqrt{at}\sqrt{2n(n + 1)} \tag{11b}$$

The exact solution [17], for example, is

$$\frac{T(x, t) - T_\infty}{(T_s - T_\infty)} = 1 - \operatorname{erf}\left(\frac{x}{2\sqrt{\alpha t}}\right) \tag{12}$$

The boundary fractional boundary flux $(\partial T/\partial x)_{fr(x=0)}$ defined by (9a) is

$$-\left(\frac{\partial T}{\partial x}\right)_{fr(x=0)} = \frac{1}{\sqrt{at}}\frac{1}{\sqrt{\pi}}(T_s - T_\infty) \tag{13}$$

Then, with the condition (7) we have

$$-\left(\frac{\partial T}{\partial x}\right)_{fr(x=0)} = -\left(\frac{\partial T}{\partial x}\right)_{a(x=0)} \quad \Rightarrow \quad \frac{1}{\sqrt{at}}\frac{1}{\sqrt{\pi}}(T_s - T_\infty) = \frac{n}{\sqrt{at}\sqrt{2n(n+1)}}(T_s - T_\infty) \tag{14}$$

That yields

$$\frac{1}{\sqrt{\pi}} = \frac{n}{\sqrt{2n(n+1)}} \quad \Rightarrow \quad n = \frac{2}{\pi - 2} \approx 1.75 \tag{15}$$

This result exactly matches that obtained by help of the exact solution (14) in [18] using EGM, as well as that developed by two integral constraints in [13]. It will be denoted hereafter as $n_0^T \approx 1.75$ to be distinguished from the exponents derived by other methods.

2.3.1. Example 2. Prescribed Flux Boundary condition at $x = 0$, $q_s''(0,t) = q_0 = const$

The HBIM approximate solution is [13]

$$T_a = T_\infty + \frac{q_s''(0,t)\delta}{\lambda n}\left(1 - \frac{x}{\delta}\right)^n \tag{16a}$$

$$\delta = \sqrt{at}\sqrt{n(n+1)} \tag{16b}$$

and the exact solution [17] expressed as

$$\frac{T_e(x,t) - T_\infty}{\frac{q_0}{\lambda}\sqrt{\alpha t}} = 2\left[i\,\mathrm{erfc}\left(\frac{x}{2\sqrt{\alpha t}}\right)\right] \tag{17}$$

The local temperature $T_{fr(x=0)}$ provided by (8) with the condition (7) yields

$$T_{fr(x=0)} = T_{a(x=0)} \quad \Rightarrow \quad 2q_s''(0,t)\frac{\sqrt{\alpha t}}{\lambda\sqrt{\pi}} + T_\infty = T_\infty + \frac{q_s''(0,t)\delta}{\lambda n} \tag{18a}$$

Then, the results is

$$\frac{2}{\sqrt{\pi}} = \frac{\sqrt{n(n+1)}}{n} \quad \Rightarrow \quad n = \frac{\pi}{(4-\pi)} \approx 3.65 \tag{18b}$$

The result (18b) is exactly the same as those developed in [18] by the EGM approach and in [13] by using the exact solutions [17]. It will be denoted hereafter as $n_0^q \approx 3.65$ to be distinguished from the exponents derived by other methods. The common complain [15] against the calibrating the profile at $x = 0$ is the value of the exponent is use further over the entire thermal layer. However, we have clearly to distinguish two situations: (1) Problems requiring solutions near the point $x = 0$ such as establishing the surface flux when the temperature is prescribed or those related to pre-heating or pre-ablation problems, i.e. the solutions of Braga [14] correspond to this group. (2) Problems related to correct determination of temperature profile across thermal layer and its front propagation – mainly defined as Stefan problems [15].

3. Mean-squared error approach in the exponent calibration

3.1. Myer's approach

Recently, Myers [15] has developed a procedure based on the Langford criterion [16]. The Myers' method looks for minimum of a function obtained after substitution of the profile (5) in the Langford criterion and expressed as

$$E_n(n,t) \equiv \int_0^{\delta(t)}\left[\frac{\partial T_a(x,t)}{\partial x^2} - \frac{1}{\alpha}\frac{\partial T_a(x,t)}{\partial t}\right]^2 \mathrm{d}x \geqslant 0 \tag{19a}$$

$$E_n(n,t) = \frac{\sqrt{\alpha}}{t\sqrt{t}}e_n(n,t) \tag{19b}$$

If $T_a(x,t)$ matches the exact solution $T_e(x,t)$, then function $E_n(n,t)$ would be identically zero. In contrast to the original work [16], where the minimum of $e_n(n,t)$ was looked for integer values of n, the Myers approach leads to no-integer values, after setting $t = 0$. The main assumption [15] is that the time-dependent terms of $e_n(n,t)$ vanish as the time goes on. The exponents obtained by this method are: $n_M^T = 2.235$ and $n_M^q = 3.854$ for the fixed temperature and fixed flux, respectively.

Table 1
Optimal exponents derived by the methods used.

Condition at $x=0$	Calculated at $x=0$		Exact solution	HBIM solutions		
				$n_0^T=1.75$	$n_M^T=2.235$	$n_\eta^T=1.5047$
Prescribed temperature problem	Calculated flux $\frac{n}{\sqrt{at}\sqrt{2n(n+1)}}(T_s-T_\infty))$	$\Rightarrow$	$0.564\frac{\Delta T}{\sqrt{at}}$	$0.564\frac{\Delta T}{\sqrt{at}}$	$0.587\frac{\Delta T}{\sqrt{at}}$	$0.548\frac{\Delta T}{\sqrt{at}}$
		Error (%)	0	0	+4.07	−2.082
				$n_0^q=3.65$	$n_M^q=3.854$	$n_\eta^q=3.314$
Prescribed flux problem	Calculated temperature $\Delta T=T_s-T_\infty=\frac{q_0}{\lambda n}\delta$	$\Rightarrow$	$1.128\frac{q_0}{\lambda}\sqrt{at}$	$1.128\frac{q_0}{\lambda}\sqrt{at}$	$1.122\frac{q_0}{\lambda}\sqrt{at}$	$1.140\frac{q_0}{\lambda}\sqrt{at}$
		Error (%)	0	0	−0.53	+1.14

The first exponents differs significantly from 1.75 defined by calibrating of the profile at $x=0$, either by the exact solution [13,18] or through fractional boundary flux (see Eq. (15)). For the prescribed flux problem $n_M^q=3.854$ is almost the same as $n_0^q=3.65$ defined at $x=0$.

3.2. Self-similarity transform approach

With $\eta=x/2\sqrt{\alpha t}$ the approximate profile can be expressed as $\Theta=(1-\eta/F)^n$, where the term F is: a) $F_T=\sqrt{2n(n+1)}$ with is a prescribed temperature and b) $F_q=\sqrt{n(n+1)}$ with a prescribed flux, respectively. With the similarity variable η the basic Eq. (1) becomes [17]

$$\frac{\partial^2\Theta}{\partial\eta^2}+2\eta\frac{\partial\Theta}{\partial\eta}=0 \tag{20}$$

The integration of (20) over the thermal penetration depth transforms the integration boundaries from $0\leqslant x\leqslant\delta$ into $0\leqslant\eta\leqslant\delta/\sqrt{\alpha t}$ (at $\delta/\sqrt{\alpha t}=F\Rightarrow\Theta=0$), and the integration over the penetration depth ($0\leqslant\eta\leqslant F$) yields

$$E_n(n)=\frac{n^2}{F^3}\frac{(n-1)^2}{(2n-3)}+\frac{4nF^2}{n(2n-1)(2n+1)}+4\frac{n^2}{F}\frac{(n-1)}{(2n-2)(2n-1)}=0 \tag{21}$$

The final equation relating the similarity variable and the parameters of the approximate profile is

$$4n^6-8n^5+3n^4+2n^3-n^2+F^5(8n-12)+F^2\left(8n^4-8n^3-6n^2\right)=0 \tag{22}$$

This approach, therefore, takes into account all terms of $E_n(n)$, unlike the method of Myers. With the specific form of F defined above we have (calculations performed with Maple 13):

- **Prescribed temperature** at $x=0$ and $F=F_T$ the derivative $\mathrm{d}E_T(n)/\mathrm{d}n=0$ at $n\gg1.194$ with $E_n(1.194)\gg194.533$, while $n=1.740$ is the only real positive zero of (25) providing $E_n(1.7405)\gg4.84$. The second real root is $n\gg-2.459$. The other two roots are: complex ones: $-0.768\pm i.0.088$. On other hand, the numerical solution provides $n=1.5047$.
- **Prescribed flux** at $x=0$ and $F=F_q$: the derivative $\mathrm{d}E_q(n)/\mathrm{d}n=0$ at $n\gg1.194$, while $n=1.487$ is the only real zero of (25). The other two roots are complex: $-0.623\pm i.101$. On other hand, the numerical solution provides, $n=3.314$.

4. Numerical examples and discussion

All method developed above provide different values of the optimal exponent of the parabolic profile.
The evaluation of the correct values will be performed in two cases:

(a) Determination of the flux at $x=0$ with the temperature is prescribed and *vice versa*.
(b) Comparisons of the approximate profiles expressed through the similarity variable η thus allowing a direct comparison with the exact solutions.

4.1. Results at $x=0$ and mean-squared errors of approximation

The determination of the optimal exponent was commented above and the final results are summarized in Table 1. Besides, Table 2 summarizes the information about the errors in approximation based on the mean-squared error approach with different exponents derived in this work.

- **Prescribed temperature** at $x=0$: The calculated surface fluxes are: $q_s''(n=1.740)\approx0.563(\Delta T/\sqrt{at})$ and $q_s''(n=1.5047)\approx0.548(\Delta T/\sqrt{at})$. The fist flux is practically that provided by the exact solution while the second one underestimates the surface flux with about 2%. Even thought the difference is practically negligible, the right exponent should be based on the value of E_n (see Table 2, too): With $n=1.740$ we have $E_n(1.7405)\approx4.84$, while $E_n(1.5047)\approx0.0431$.

Table 2
Mean-squared error function $E(n)$ of approximation.

Condition at $x=0$	Error function		HBIM solutions		
Prescribed temperature			$n_0^T = 1.75$	$n_M^T = 2.235$	$n_\eta^T = 1.5047$
	$E(n)$	$\Rightarrow$	2.517	2.191	0.0431
Prescribed flux			$n_0^q = 3.65$	$n_M^q = 3.854$	$n_\eta^q = 3.314$
	$E(n)$	$\Rightarrow$	0.0394	0.0604	$\approx 1.1 \times 1^{-7}$

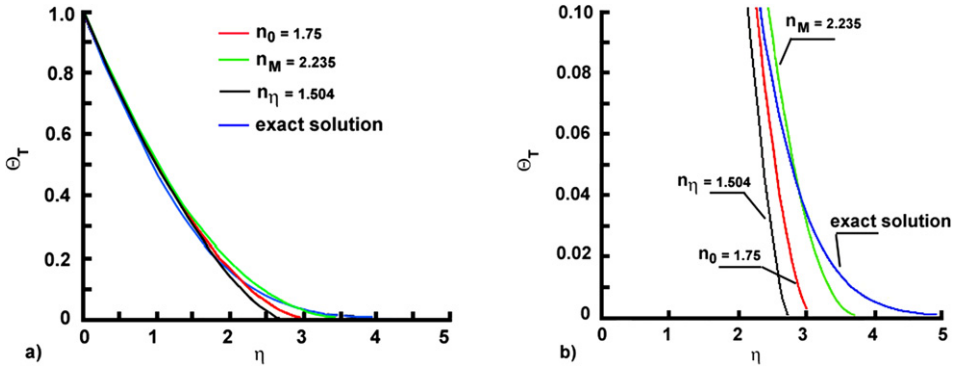

Fig. 1. Temperature profiles with the prescribed temperature problem. (a) Approximate profiles over the range $0 \leqslant \eta \leqslant 5$. (b) Approximate profiles close to the edge of the thermal layer, $3 \leqslant \eta \leqslant 5$.

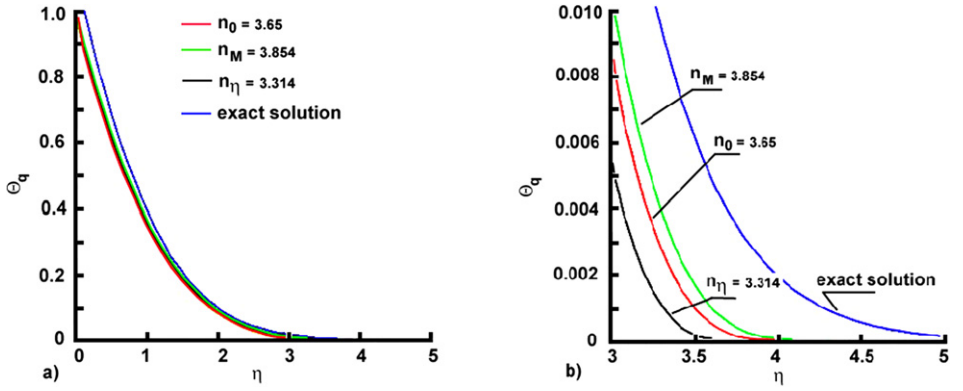

Fig. 2. Temperature profiles with the prescribed flux problem. (a) Approximate profiles over the range $0 \leqslant \eta \leqslant 5$. (b) Approximate profiles close to the edge of the thermal layer, $3 \leqslant \eta \leqslant 5$.

- **Prescribed flux:** Simple calculations of the temperature at $x=0$ with $n=1.487$ provide: $T_s \approx 1.293(q_0/\lambda)\sqrt{at}$ that overestimates the exact solution with about 14.62% and gives $E_n(1.497) \approx 0.0092$ (see Table 1 and Table 2). In contrast, with $n=3.314$ we have: $T_s \approx 1.140(q_0/\lambda)\sqrt{at}$, i.e. with about +1.14% error, and E_n is practically zero (see Table 2).

Therefore, the optimal exponents are with the mean-squared error approach using the similarity variable are: $n_\eta^T \approx 1.5047$ and $n_\eta^q \approx 3.314$. The Myer's exponents n_M^T and n_M^q satisfy the domain condition to minimize the mean-squared error over the entire thermal penetration depth but under the *ad hoc* accepted condition that the time-dependent terms of $E(n,t)$ should be excluded from the minimization procedure; a step eliminated in the similarity approach developed in this work.

4.2. Approximate profiles

The approximate profiles obtained with the parabolic profiles using with different exponents are illustrated in Figs. 1 and 2. In general, the approximate profiles are quite close to the exact solutions when $0 \leqslant \eta \leqslant 2$ and discrepancies becomes more evident when $3 \leqslant \eta \leqslant 5$. The former range corresponds to zones close to point $x=0$ while the second one to the front of the penetration layer ($x \to \delta$). In this context, regarding the fixed exponents defined above, the higher value of n, the higher upper limit for η, because at $\eta = F(n)$ the approximate profiles end. Hence, looking at the values of exponents in Table 1, it is clears that those provided by Myers allow the approximate profiles to be extended towards larger values of η

beyond those at which the others (with lower exponents end) end (cross the abscissa). This is only reason why the profiles calculated by the Myers' exponents continue together the exact solutions towards zero in ranges where the other profiles provides negative unrealistic values. The additional plots in Figs. 1 and 2 show through "a magnifying glass" the behavior of the approximated solution in narrow ranges of variations of η. In all cases, irrespective of the method determining the profile exponent, the approximate profiles underestimate the exact temperature profiles. These plots reveal that the approximate solutions work almost equally for $0 < \eta < 1$ when the prescribed temperature problem is simulated and within the range $0 < \eta < 3.5$ for the flux problem. In this context, Braga [23], has commented that the profiles with $n_0^T = 1.75$ and $n_0^q = 3.65$ work quite well up to $\eta \approx 4$ and the differences with the exact solution are undetectable; a conclusion that matches the outcomes of the present work.

5. Conclusions

The calibration problem of the integral-balance parabolic profile with unspecified exponent was investigated with three techniques: (1) Additional boundary conditions at $x = 0$ created by entropy generation minimization (EGM) conditions and provided by half-time a fractional derivative (integral); (2) The Myers' approach; and (3) Similarity transform approach developed in the present work looking for optimal exponent minimizing the mean-squared error the domain equation over the thermal penetration layer.

The main outcomes can be outlined as:

- The EGM approach is clear and straightforward since it generates an additional boundary condition to the approximate profile that can be easily provided by fractional (Riemann–Liouville) half-time derivative (prescribed flux problem) or integral (prescribed temperature problem). These boundary conditions do not exist in the classical method of Goodman.
- The Myers approach is based on the classic L_2 norm but leads to cumbersome expressions including both the exponent and the time. The crucial point of this approach is the omission of the time-dependent terms. The method provides the highest values of the profile exponent among the others.
- The similarity approach (SA) transforms the domain equation, following also the rules of the L_2 norm, but leads to simple expression of the mean-squared error over the thermal layer. The determination of the optimal exponent by SA is straightforward. The values are between those determined by the EGM and Myers.
- All methods provide approximate profiles that almost match the exact solution in the range $0 \leqslant \eta \leqslant 2$. The discrepancies become more significant as the point approaches the front of the thermal layer. This a general drawback of the HBIM using a fixed exponent over the entire domain $0 \leqslant \delta \leqslant$. The approximation can be improved by the concept of the self-adaptive exponent of the parabolic profile developed in the companion article (Part 2) [24].
- The use of fractional half-time semi-derivative is a step ahead toward improvement of the HBIM approach never applied so far. The fractional calculus approach has a great potential in solving practical engineering problems in a broad aspect [25–30] avoiding cumbersome entire-domain analytical solutions. The example developed in this work may serve as a good source of ideas to solve many practical problems such as thermal contact resistance [31,32] as it was demonstrated in [33].

Acknowledgements

The work was supported by the grant N10852/2011 of Univ. Chemical Technology and Metallurgy (UCTM), Sofia, Bulgaria.

References

[1] T. R Goodman, The heat balance integral and its application to problems involving a change of phase, Trans. ASME 80 (1–2) (1958) 335–342.
[2] A.S. Wood, F. Mosally, A. Al-Fhaid, On high-order polynomial heat-balance integral implementations, Thermal Science 13 (2) (2009) 11–25.
[3] V. Novozhilov, Application of heat-balance integral method to conjugate thermal explosion, Thermal Science 13 (2) (2009) 73–80.
[4] N. Sadoun, El-Khider Si-Ahmed, P. Collinet, J. Legrand, On the Goodman heat-balance integral method for Stefan-like problems, Thermal Science 13 (2) (2009) 91–96.
[5] S.K. Sahu, P.K. Das, S. Bhattacharyya, How good is Goodman's heat-balance integral method for analyzing the rewetting of hot surfaces? Thermal Science 13 (2) (2009) 97–112.
[6] B. Baudouy, Heat-balance integral method for heat transfer in superfluid helium, Thermal Science 13 (92) (2009) 121–132.
[7] J.A. Esfahani, S. Koohi-Fayegh, Entropy generation analysis in error estimation of an approximate solution: A constant surface temperature semi-infinite conductive problem, Thermal Science 13 (2) (2009) 133–140.
[8] A.P. Roday, M.J. Kazmierczak, Analysis of phase-change in finite slabs subjected to convective boundary conditions: Part I – Melting, Int. Rev. Chem. Eng. 1 (1) (2009) 87–99.
[9] A.P. Roday, M.J. Kazmierczak, Analysis of phase-change in finite slabs subjected to convective boundary conditions: Part II – Freezing, Int. Rev. Chem. Eng. 1 (1) (2009) 100–108.
[10] T.R. Goodman, Application of integral methods to transient nonlinear heat transfer, Adv. Heat Transfer 1 (1964) 51–122.
[11] S.K. Sahu, P.K. Das, S. Bhattacharyya, A comprehensive analysis of conduction-controlled rewetting by the heat balance integral method, Int. J. Heat Mass Transfer 49 (2006) 4978–4986.
[12] J. Hristov, An inverse Stefan problem relevant to boilover: Heat balance integral solutions and analysis, Thermal Science 11 (2) (2007) 141–160.
[13] J. Hristov, The heat-balance integral method by a parabolic profile with unspecified exponent: Analysis and benchmark exercises, Thermal Science 13 (2) (2009) 22–48.

[14] W. Braga, M. Mantelli, A new approach for the heat balance integral method applied to heat conduction problems, in: 38th AIAA Thermophysics Conference, Toronto, Ontario, June 6–9, 2005, paper AIAA-2005-4686.
[15] T. Myers, Optimizing the exponent in the hear balance and refined integral methods, Int. Comm. Heat Mass Transfer 36 (2009) 143–147.
[16] D. Langford, The heat balance integral method, Int. J. Heat Mass Transfer 16 (1973) 2424–2428.
[17] H.S. Carslaw, J.C. Jaeger, Conduction of Heat in Solids, 2nd ed., Oxford University Press, Oxford, UK, 1992.
[18] J. Hristov, Research note on a parabolic heat-balance integral method with unspecified exponent: An entropy generation approach in optimal profile determination, Thermal Science 13 (2) (2009) 49–59.
[19] Z. Kolenda, J. Donizak, J. Hubert, On the minimum entropy production in steady state heat conduction processes, Energy 29 (2004) 2441–2460.
[20] K.B. Oldham, J. Spanier, The Fractional Calculus, Academic Press, New York, 1974.
[21] V.V. Kulish, J.L. Lage, Fractional-diffusion solutions for transient local temperature and heat flux, J. Heat Transfer 122 (2000) 372–376.
[22] L. Debnath, Nonlinear Partial Differential Equations for Scientist and Engineers, Birkhauser, Boston, 1997.
[23] W.F. Braga, Integral method and electrical analogy to solution of heat transfer in ablating solids, MsS Thesis, Federal University of Santa Catarina, Florianópolis, Brazil, 2002 (in Portuguese).
[24] J. Hristov, The heat-balance integral: 2. Parabolic profile with a variable exponent: the concept, analysis and numerical experiments, C. R. Mecanique 340 (7) (2012) 493–500.
[25] I. Siddique, D. Vieru, Stokes flows of a Newtonian fluid with fractional derivatives and slip at the wall, Int. Rev. Chem. Eng. 3 (2011) 822–826.
[26] H. Qi, M. Xu, Some unsteady unidirectional flows of a generalized Oldroyd-B fluid with fractional derivative, Appl. Math. Model. 33 (2009) 4184–4191.
[27] M.C. dos Santos, E. Lenzi, E.M. Gomes, M.K. Lenzi, E.K. Lenzi, Development of heavy metal sorption isotherm using fractional calculus, Int. Rev. Chem. Eng. 3 (2011) 814–817.
[28] J. Hristov J, Starting radial subdiffusion from a central point through a diverging medium (a sphere): heat-balance integral method, Thermal Science 15 (2011) S5–S20.
[29] R.A. Pfaffenzeller, M.K. Lenzi, E.K. Lenzi, Modeling of granular material mixing using fractional calculus, Int. Rev. Chem. Eng. 3 (2011) 818–821.
[30] R.P. Meilanov, M.R. Shabanova, E.N. Akhmedov, A research note on a solution of Stefan problem with fractional time and space derivatives, Int. Rev. Chem. Eng. 3 (2011) 810–813.
[31] M. Bouneder, M. El Ganaoui, B. Pateyron, P. Fauchais, Relevance of a thermal contact resistance depending on the solid/liquid phase change transition for sprayed composite metal/ceramic powder by direct current plasma jets, C. R. Mécanique 336 (7) (2008) 592–599.
[32] H. Belghazi, M. El Ganaoui, J.C. Labbe, Analytical solution of unsteady heat conduction in a two-layered material in imperfect contact subjected to a moving heat source, Int. J. Thermal Sciences 49 (2) (2010) 311–318.
[33] J. Hristov, Thermal impedance at the interface of contacting bodies: 1-D example solved by semi-derivatives, Thermal Science 16 (2) (2012), doi:10.2298/TSCI111125017H.